Available online at www.sciencedirect.com

ScienceDirect

Ceramics International 40 (2014) 1205–1208

CERAMICS INTERNATIONAL

www.elsevier.com/locate/ceramint

Short communication

Shape-controlled electrochemical synthesis of $SrWO_4$ crystallites and their optical properties

Xuyun Li, Zuwei Song*, Baohan Qu

School of Chemistry and Pharmaceutical Science, Qingdao Agricultural University, Qingdao 266109, PR China

Received 21 April 2013; received in revised form 18 May 2013; accepted 27 May 2013
Available online 31 May 2013

Abstract

$SrWO_4$ crystallites with various morphologies were synthesized simply by adjusting electrolyte composition in an electrochemical-assisted precipitation process. The structure and morphology characterization of the products were investigated by X-ray diffraction (XRD) and field emission scanning electron microscopy (FESEM). Results indicate that spindle-like, pillar-/needle-like and flower-like $SrWO_4$ crystallites with scheelite structure can be obtained by respectively introducing ethylene glycol (DEG), ethanol (EG) and polyethylene glycol (PEG400) into the electrolyte. Ultraviolet–visible (UV–vis) adsorption spectra and photoluminescence (PL) spectra have shown that the optical properties of the products are greatly influenced by their morphologies. $SrWO_4$ flowers exhibit the strongest absorption ability in UV region and the weakest photoluminescence intensity centered at about 475 nm.

Keywords: C. Optical properties; $SrWO_4$; Electrochemical synthesis

1. Introduction

In the field of inorganic material, the structure design, dimension control and morphology optimization have recently been viewed as the challenging issues [1]. And for achieving enhanced performance or amazing properties superior to their bulk counterparts, great efforts have been focused on the controlled synthesis of novel micro- and nanostructures with uniform size and shape [2,3].

As an optoelectronic material, $SrWO_4$ was originally used as photoluminescence medium and lasers hosts, but recently their promising application in optical fibers, photocatalyst and antibacterial materials has attracted much interest [4–6]. To date, except for czochralski technique and pulsed laser deposition [7,8], wet-chemistry routes including precipitation [9], polymeric precursor [10], solvothermal [11], microwave radiation [12,13] and microemulsion-mediated method [14] have been reported to prepare $SrWO_4$ crystals. Considering energy savings and environmentally benign design, the electrochemical route undoubtedly has an advantage over the above ones, but the existing literature mainly focuses on the deposition of $SrWO_4$ film [15,16].

Herein, by using a simple electrochemical-assisted precipitation method, $SrWO_4$ with diverse morphologies, including octahedron, spindle, pillar, needle, flower and nanoparticle was synthesized. The effects of solvent type on the crystallization process and the relationship between morphology and UV–vis absorption ability as well as PL property were also investigated. To the best of our knowledge, there have been no reports on the shape-controlled preparation of $SrWO_4$ crystallites by appropriately incorporating organic additive into the electrochemical synthesis system.

2. Experimental procedure

The electrochemical synthesis system, as shown in Fig. 1, is composed of a DC power supply, a 150 mL Teflon beaker (electric tank) and two metal electrodes with the same dimension (50 mm × 20 mm × 0.1 mm) and high purity (99.5%). The pretreated tungsten sheet and platinum sheet

*Corresponding author. Tel.: +86 532 86080374; fax: +86 532 86080213.
E-mail addresses: cataszw@hotmail.com, fushiyufanghu@sina.cn (Z. Song).

0272-8842/$ - see front matter © 2013 Elsevier Ltd and Techna Group S.r.l. All rights reserved.
http://dx.doi.org/10.1016/j.ceramint.2013.05.102

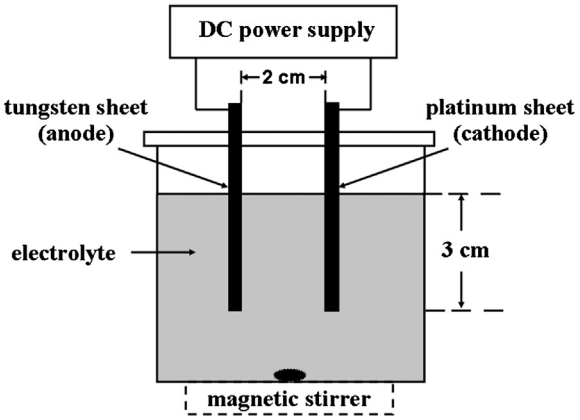

Fig. 1. The schematic diagram of the electrochemical synthesis system.

were used as an anode and a cathode, respectively. All electrolytes were prepared from analytical grade reagents. In a typical procedure, 0.005 mol $Sr(NO_3)_2$ was dissolved into 100 mL distilled water or mixed solvent composed of 80 mL distilled water and 20 mL DEG, EG and PEG400, respectively. 0.2 M NaOH or HCl solution was added drop wise to adjust the solution pH value to 10. Afterward, two electrodes were parallelly immersed into the electrolyte solution for 3 cm and kept 2 cm away from each other, followed by the electrochemical reaction at 1.0 A for 5 min with magnetic stirring. Finally, a precipitate was harvested by centrifugation, washed and dried at ambient temperature.

The crystal structure and crystallinity of the product were characterized by an X-ray diffractometer (XRD, Bruker D8) using Cu Kα radiation. The microstructure of the product was analyzed by field emission scanning electron microscopy (FESEM, JSM-7500). UV–vis adsorption property was taken on a spectrophotometer (UV–vis, TU1901) with an integrating sphere attachment. Photoluminescence spectra were recorded by using a fluorescence spectrometer (PL, Fluorolog-3) with an excitation wavelength of 290 nm.

3. Results and discussion

Fig. 2 shows XRD patterns of samples synthesized in different electrolyte solutions. All the diffraction peaks can be indexed to scheelite-type tetragonal $SrWO_4$ (JCPDS no. 08-0490), demonstrating that $SrWO_4$ crystallites can be rapidly prepared in all cases. Moreover, their crystallization seems to be sensitive to the kind of solvent. When using water as the only solvent, the weakest intensity emerged corresponding to their poorest crystallinity. With the decline of dielectric constant from H_2O to DEG, EG and PEG400, the intensity of the diffraction peaks becomes stronger, meaning that the crystallinity gradually increased. In addition, the presence of EG in the synthetic system may promote an orientation growth, as confirmed from the larger relative intensity of the (204)/(112) than that of the other three samples.

Fig. 3 shows SEM micrographs of $SrWO_4$ crystallites obtained in different electrolyte solutions. Evidently, the morphology of the product was found to be tunable by varying

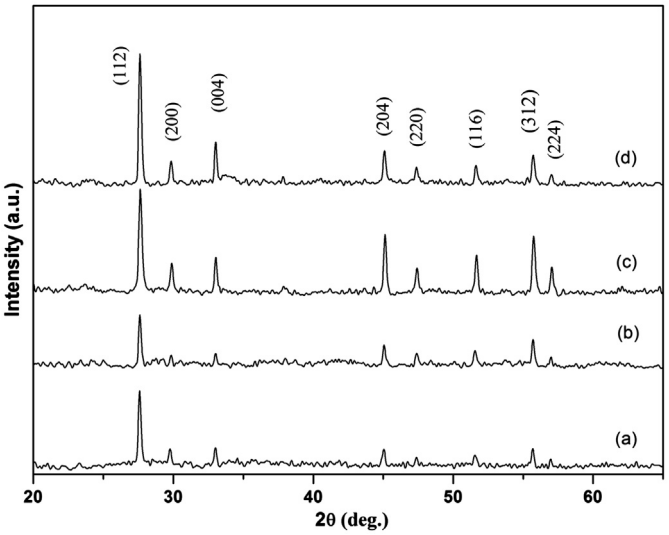

Fig. 2. XRD patterns of samples prepared with different solvent: (a) H_2O, (b) H_2O–DEG, (c) H_2O–EG and (d) H_2O–PEG400.

the introduced agents. Without using organic additives, $SrWO_4$ micro-octahedrons with size of 1–2 μm and rough surface can be obtained (Fig. 3(a)), indicating their poor crystallinity. Different from the shuttle-like particles with higher surface defect concentration (Fig. 3(b)), needle-/pillar-like crystallinites (Fig. 3(c)) were prepared in H_2O–EG system, showing an aspect ratio of about 10–20 which is larger than that of the former. Moreover, high magnification picture (Fig. 3(d)) revealed that $SrWO_4$ pillars are composed of a large amount of oval-like subgrains with size less than 100 nm. These nanoparticles connected with each other to form pillar architecture with recognizable boundaries. In H_2O–PEG400 electrolyte, flower-like compositional architectures with high crystallinity and diameter of 0.3–1 μm came into appearance (Fig. 3(e)). And as seen from Fig. 3(f), some flowers derived from the aggregation growth of nanosized primary particles. SEM observations confirm the great influence of additives on the crystal habit of $SrWO_4$ crystallites, consistent with XRD analysis.

In an electrochemical process, the formation of $SrWO_4$ results from the electrostatic interaction between Sr^{2+} and WO_4^{2-} ions. The amount of WO_4^{2-} produced by anode oxidation is constant at a given pH value and electric current for a certain reaction time. Actually, the added DEG, EG and PEG400 do not take part in the reaction, but its presence would change the supersaturation degree of solution and affect the nucleation and growth habit guided by Ostwald ripening process [17]. In addition, the adsorption ability of H_2O, DEG, EG and PEG400 on the particle surface is diverse due to their different dielectric constants, which may affect the self-assembled ability of the primary particles and ultimately result in different shapes [18]. The similar results can also be seen in the reference [19], where $SrWO_4$ microcrystals with rice-, star-, flower- and urchin-like shapes were prepared by a hot-injection technique through the self-assembly process of small nanocrystals, companied by the increase of height and width of $SrWO_4$ crystallites.

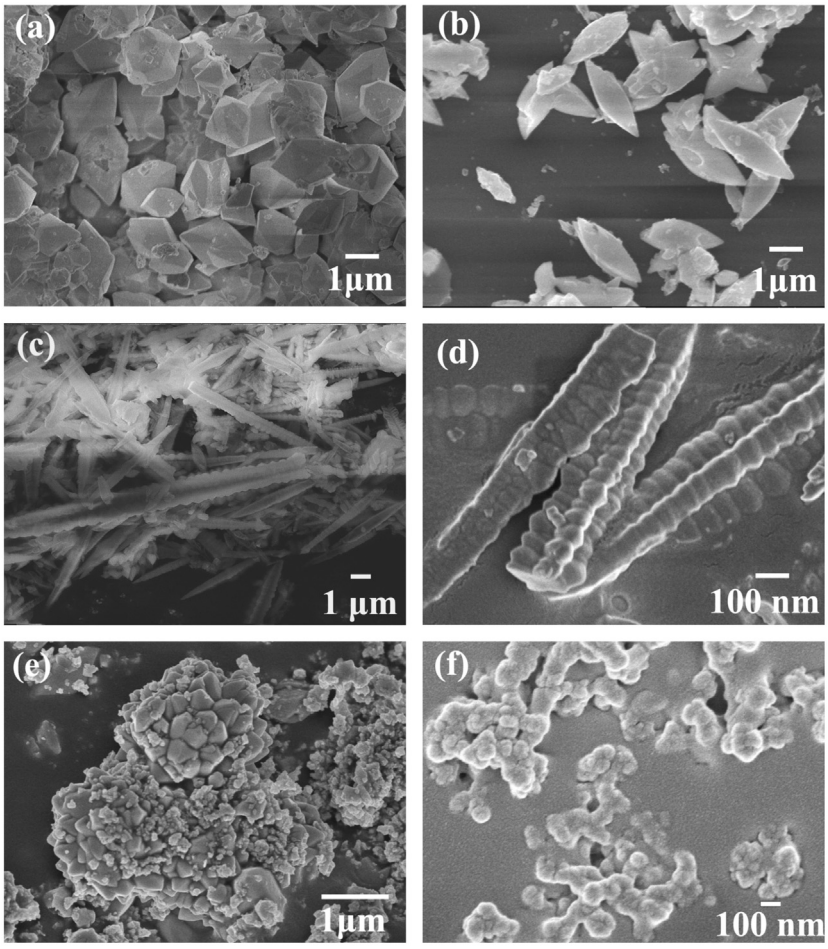

Fig. 3. FESEM images of $SrWO_4$ crystallites obtained with different solvents: (a) H_2O, (b) H_2O–DEG, (c) H_2O–EG and (e) H_2O–PEG400; (d) and (f) are amplificatory SEM image of (c) and (e), respectively.

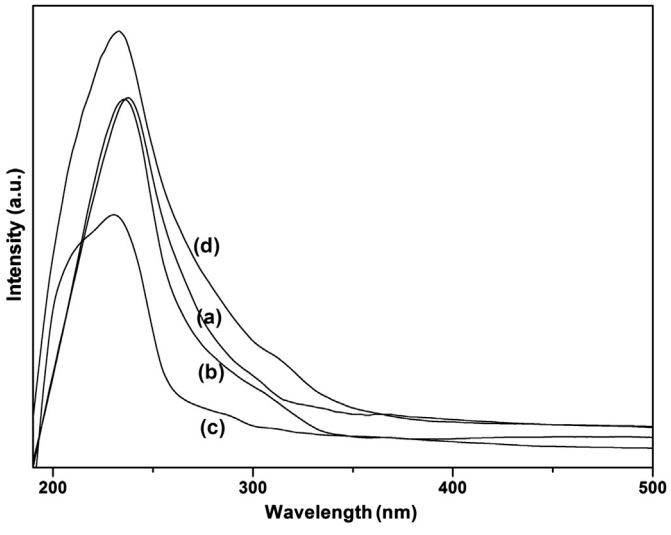

Fig. 4. UV–vis spectra of $SrWO_4$ crystallites obtained with different solvents: (a) H_2O, (b) H_2O–DEG, (c) H_2O–EG and (d) H_2O–PEG400.

The UV–vis adsorption spectra of the prepared $SrWO_4$ samples are displayed in Fig. 4. The absorption occurs mainly in ultraviolet region, exhibiting a typical optical absorption behavior of a wide-band-gap semiconducting oxide. Among all of the samples, $SrWO_4$ flowers present the highest intensity centered at 240 nm (Fig. 3(d)), and the band absorption edge is determined to be 300 nm, which shift red of about 10 nm, 20 nm and 35 nm compared with $SrWO_4$ micro-octahedrons, shuttles and pillars, respectively. Their corresponding band gaps E_g values are 4.13 eV, 4.28 eV, 4.43 eV and 4.68 eV, based on $E_g = 1240/\lambda$ [20]. The diversity of E_g can be attributed to factors such as crystallinity, shape, particle morphology, size distribution and preparation method as well [21].

Fig. 5 shows room temperature PL spectra of $SrWO_4$ crystallites with different morphologies. It can be seen that all samples exhibit an emission peak centered at 475 nm. Compared with octahedron-like and shuttle-like ones, $SrWO_4$ pillars with larger aspect ratio present the strongest PL intensity (Fig. 5(c)), corresponding to the higher recombination rate of photo-generated electrons and holes [22]. Whereas $SrWO_4$ flowers with the similar crystallinity as $SrWO_4$ pillars display the lowest PL intensity (Fig. 5(c)), implying that only a few electrons and holes can be excited by light probably due to their wide band gap and special structure. The results reveal that morphological characteristics of $SrWO_4$ have great impact

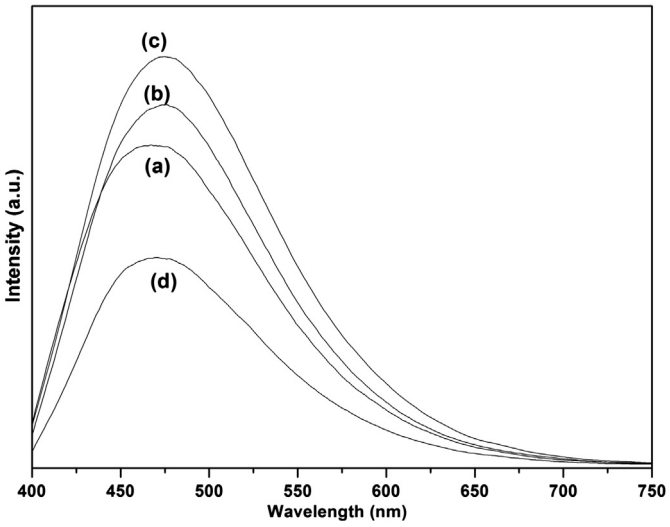

Fig. 5. PL spectra of $SrWO_4$ crystallites synthesized with different solvents: (a) H_2O, (b) H_2O–DEG, (c) H_2O–EG and (d) H_2O–PEG400.

on their PL property except for crystallinity, consistent with the UV–vis results.

4. Conclusions

$SrWO_4$ micro-octahedrons, shuttles, pillars and flowers were controllably prepared via a facile electrochemical process in different electrolytes. The PL spectra together with the UV–vis, SEM and XRD results indicate the presence of organic additives can change the supersaturation degree of the electrolyte and crystallization habit of the samples, which can lead to the variety of the shape, size and crystallinity of $SrWO_4$ crystallites, and eventually result in the diversity of their optical properties.

Acknowledgment

This work was supported by the Natural Science Foundation of Shandong Province (No. ZR2012EMM017) and Scientific Research Foundation for Advanced Scholars of Qingdao Agricultural University (No. 631022).

References

[1] A.L. Tiano, C. Koenigsmann, A.C. Santullia, S.S. Wong, Solution-based synthetic strategies for one-dimensional metal-containing nanostructures, Chemical Communications 46 (2010) 8093–8130.
[2] Tamiko Kinoshita, Mamoru Senna, Yutaka Doshida, Hiroshi Kishi, Synthesis of size controlled phase pure $KNbO_3$ fine particles via a solid-state route from a core-shell structured precursor, Ceramics International 38 (2012) 1897–1904.
[3] A. Paulraj, P. Natarajan, K. Munnisamy, M.K. Nagoor, K.P. Nattar, B. Abdulrazak, J. Duraisamy, Photoluminescence efficiencies of nanocrystalline versus bulk Y_2O_3:Eu phosphor-revisited, Journal of the American Ceramic Society 94 (2011) 1627–1633.
[4] J. Sulc, H. Jelnkova, T.T. Basiev, M.E. Doroschenko, L.I. Ivleva, V. V. Osiko, P.G. Zverev., Nd:$SrWO_4$ and Nd:$BaWO_4$ Raman lasers, Optical Materials 30 (2007) 195–197.
[5] D. Errandonea, C. Tu, G. Jia, I.R. Martin, U.R. Rodrguez-Mendoza, F. Lahoz, M.E. Torres, V. Lavn, Effect of pressure on the luminescence properties of Nd^{3+} doped $SrWO_4$ laser crystal, Journal of Alloys and Compounds 451 (2008) 212–214.
[6] Z.C. Shan, Y.M. Wang, H.M. Ding, F.Q. Huang, Structure-dependent photocatalytic activities of MWO_4 (M=Ca, Sr, Ba), Journal of Molecular Catalysis A: Chemical 302 (2009) 54–58.
[7] Z.C. Ling, H.R. Xia, D.G. Ran, F.Q. Liu, S.Q. Sun, J.D. Fan, H.J. Zhang, J.Y. Wang, L.L. Yu, Lattice vibration spectra and thermal properties of $SrWO_4$ single crystal, Chemical Physics Letters 426 (2006) 85–90.
[8] J.Y. Huang, Q.X. Jia, Structural properties of $SrWO_4$ films synthesized by pulsed-laser deposition, Thin Solid Films 444 (2003) 95–98.
[9] Di Chen, Zhe Liu, Shuxin Ouyang, Jinhua Ye, Simple room-temperature mineralization method to $SrWO_4$ micro/nanostructures and their photocatalytic properties, The Journal of Physical Chemistry C 115 (2011) 15778–15784.
[10] E. Orhan, M. Anicete-Santos, M.A.M.A. Maurera, F.M. Pontes, C. O. Paiva-Santos, A.G. Souza, J.A. Varela, P.S. Pizani, E. Longo, Conditions giving rise to intense visible room temperature photoluminescence in $SrWO_4$ thin films: the role of disorder, Chemical Physics 312 (2005) 1–9.
[11] T. Thongtem, A. Phuruangrat, S. Thongtem, Preparation and characterization of nanocrystalline $SrWO_4$ using cyclic microwave radiation, Current Applied Physics 8 (2008) 189–194.
[12] J.C. Sczancoski, L.S. Cavalcante, M.R. Joyaa, J.W.M. Espinosa, P. S. Pizani, J.A. Varela, E. Longo, Synthesis, growth process and photoluminescence properties of $SrWO_4$ powders, Journal of Colloid and Interface Science 330 (2009) 227–236.
[13] T. Thongtem, S. Kaowphong, S. Thongtem, Influence of cetyltrimethylammonium bromide on the morphology of AWO_4 (A=Ca, Sr) prepared by cyclic microwave irradiation, Applied Surface Science 254 (2008) 7765–7769.
[14] Z. Chen, Q. Gong, J. Zhu, Y.P. Yuan, L.W. Qian, X.F. Qian, Controllable synthesis of hierarchical nanostructures of $CaWO_4$ and $SrWO_4$ via a facile low-temperature route, Materials Research Bulletin 44 (2009) 45–50.
[15] W.S. Cho, M. Yashima, M. Kakihana, A Kudo, T Sakata, M. Yoshimura, Room-temperature preparation of highly crystallized luminescent $SrWO_4$ film by an electrochemical method, Journal of the American Ceramic Society 78 (1995) 3110–3112.
[16] C. Cui, J. Bi, D. Gao, Room temperature synthesis of crystallized luminescent $SrWO_4$ films by an adjustable galvanic cell method, Journal of Crystal Growth 310 (2008) 4385–4389.
[17] S.F. Chen, S.H. Yu, J. Jiang, F.Q. Li, Y.K. Liu, Polymorph discrimination of $CaCO_3$ mineral in an ethanol/water solution: formation of complex vaterite superstructures and aragonite rods, Chemistry of Materials 18 (2006) 115–122.
[18] R.L. Penn, J.F. Banfiel, Morphology development and crystal growth in nanocrystalline aggregates under hydrothermal conditions: insights from titania, Geochimica et Cosmochimica Acta 63 (1999) 1549–1554.
[19] L.S. Cavalcante, N.C. Batista, E. Longo, J.A. Varela, M.O. Orlandi, Growth mechanism and photocatalytic properties of $SrWO_4$ microcrystals synthesized by injection of ions into a hot aqueous solution, Advanced Powder Technology 65 (2013) 159–164.
[20] K.M. Reddy, S.V. Manorama, A.R. Reddy, Bandgap studies on antase titanium dioxide nanoparticles, Materials Chemistry and Physics 78 (2002) 239–245.
[21] J.C. Sczancoski, L.S. Cavalcante, M.R. Joya, J.A. Varela, P.S. Pizani, E. Longo., $SrMoO_4$ powders processed in microwave-hydrothermal: synthesis, characterization and optical properties, Journal of Chemical and Engineering 140 (2008) 632–637.
[22] N.Q. Wu, J. Wang, D.N. Tafen, H. Wang, J.G. Zheng, J.P. Lewis, X. G. Liu, S.S. Leonard, A. Manivannan, Shape-enhanced photocatalytic activity of single crystalline anatase TiO_2 (101) nanobelts, Journal of the American Chemical Society 132 (2010) 6679–6685.